Appendix for: A new model for the HPA axis explains dysregulation of stress hormones on the timescale of weeks, Karin et al.

Contents

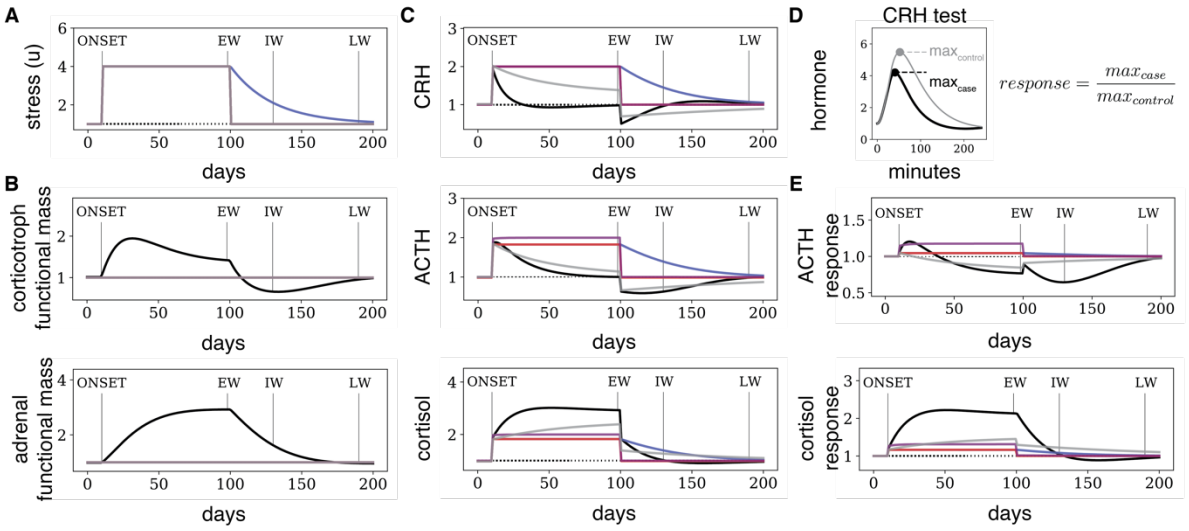

Appendix Figure S1. Model dynamics of HPA axis after prolonged stress. Numerical solutions of the HPA models after a prolonged pulse of stress input, as in Figure 3 of the main text. The model with gland functional mass dynamics (black lines) recapitulates the dynamics observed in Figure 1. Models in which mass is constant (red lines) or models with constant masses and (i) month-timescale drop in input signal (blue lines), (ii) acquisition of glucocorticoid resistance (purple lines), do not develop a blunting of ACTH responses or a mismatch between ACTH and cortisol dynamics. A model with (iii) desensitization of cortisol clearance rate (gray line) does develop a blunting of ACTH responses, but does not recapitulate the mismatch observation that ACTH dynamics normalize after cortisol dynamics.

Section 1. Several alternative models for slow timescale dynamics do not explain observed mismatch between ACTH and cortisol.

In this section we tested whether alternative models can explain the observations at the focus of this study, presented in Figure 1: blunting of ACTH responses to CRH challenges after prolonged activation of the HPA axis, which persists for weeks-months after cortisol levels and dynamics normalize. Since this persistence occurs on the timescale of weeks-months, it cannot be explained by standard hormone dynamics with a timescale of hours (red lines in Figure S1). We thus explored alternative models without gland mass dynamics, but with a relevant timescale on the order of weeks-months. The models are described in the Methods section. The model dynamics are depicted with colored lines in Figure S1, with the mass-change model of the main text in thick black line for comparison. None of the alternative models has mass changes so that the dynamics in Figure S1B,C are flat, and all lines overlap.

The first alternative model that we explored is a model where the input signal drops gradually (Methods, blue line in Figure S1A). In this model, prolonged activation of the HPA axis does not result in blunted ACTH responses, but instead in elevated ACTH levels and responses (Figure S1CE, blue lines). Moreover, the recovery of ACTH and cortisol is coordinated in this model and there is no mismatch.

A second alternative model is glucocorticoid resistance which depends on cortisol levels (Cohen *et al*, 2012; Merkulov *et al*, 2017). We model this mechanism by adding a cortisol-dependent decrease in the sensitivity of the GR (Methods, purple lines in Figure S1). This mechanism also does not result in

blunted ACTH responses (in fact, it sensitizes ACTH responses), and there is no mismatch between cortisol and ACTH after recovery from prolonged stress. The reason for this is that varying GR sensitivity does not disrupt the correspondence between ACTH levels and responses to cortisol levels, so when ACTH responses are blunted, cortisol levels are low, and vice versa.

Finally, we considered a mechanism that can reproduce persistent blunting of ACTH – a putative cortisol-dependent drop in cortisol clearance rate (Methods, gray lines in Figure S1). While this mechanism reproduces both persistent blunting and hypercortisolemia after chronic stress (Figure S1E gray lines), it does not show a mismatch between the recovery of cortisol and that of ACTH (they both recover together), and therefore it cannot explain the data of Figure 1.

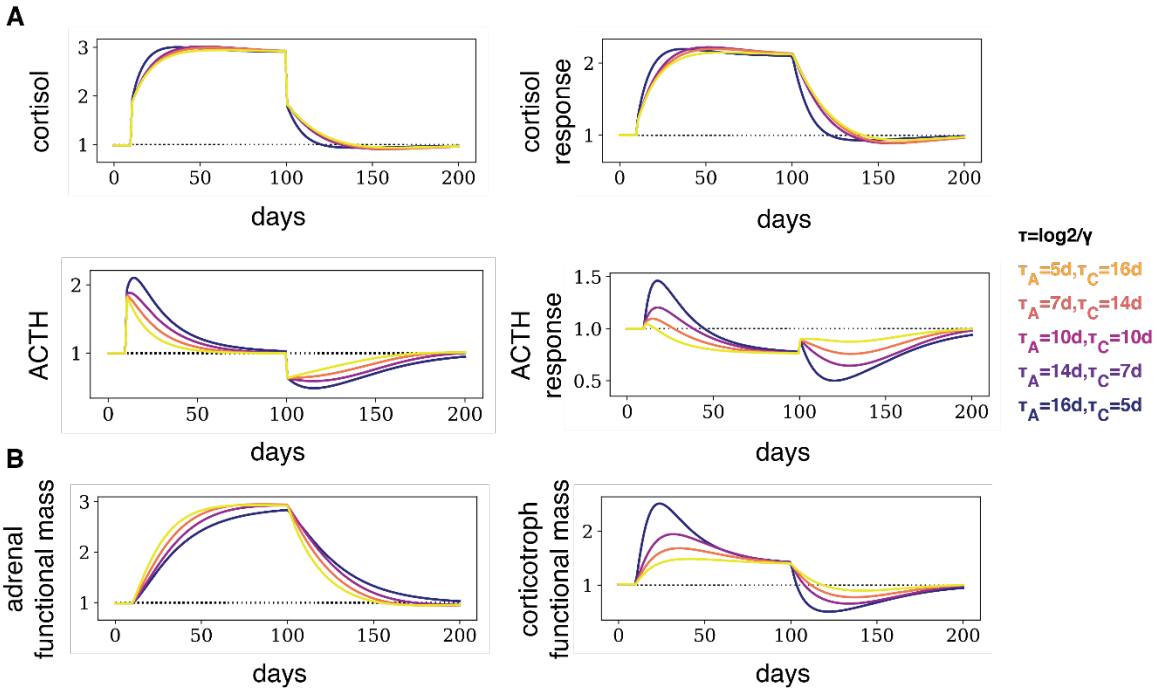

Appendix Figure S2. Model dynamics for various turnover rates of pituitary corticotrophs and adrenal cortex cells. (AB) Here we show the dynamics of the HPA axis during and after a prolonged pulse of stress, described in Figure 3, for various values of τ_A (adrenal half-life) and γ_C (corticotroph turnover). The faster the turnover of the corticotrophs relative to the turnover of the adrenal cortex, the more pronounced is the dysregulation of ACTH dynamics after prolonged stress. On the other hand, a faster turnover of corticotrophs also causes a faster return to baseline of cortisol levels and responses. For all parameter values, however, ACTH always recovers after cortisol and CRH after prolonged stress.

Appendix Section 2. Dependence of recovery from prolonged stress on corticotroph and adrenal turnover rate parameters.

We tested whether the qualitative features we discuss are robust to changes in model parameters. We note that all fast-timescale parameters (namely the hormone removal rates w_1,w_2,w_3 and specific production rates k_1,k_2,k_3) do not affect the slow timescale of weeks. The two parameters that do affect the weeks-timescale are the *turnover parameters* of the functional masses of the corticotrophs and the adrenal cortex, w_C, w. To illustrate the dependence on these two parameters, we plotted in Figure S2 the dynamics of the HPA axis variables with different values of the parameters. For ease of interpretation, we present this in terms of tissue half-lives ($\tau_C = \frac{\log 2}{w_C}, \tau_A = \frac{\log 2}{w_A}$). We find that for half-lives in the range of a few days to a few weeks, the dynamics of the HPA axis show the same qualitative features that we discussed: a return to baseline cortisol levels and CRH-test responses within a few weeks, and a return to baseline of ACTH level and responses only later, within a few months. This holds regardless of whether the corticotrophs have a faster or slower half-life than the adrenal cortex. However, the faster the turnover of the corticotrophs is compared with that of the adrenal cortex ($\tau_C \ll \tau_A$), the more severe is the blunting of ACTH in the weeks following the cessation of the stressor. On

the other hand, a faster turnover of corticotrophs also leads to faster recovery of cortisol, suggesting a tradeoff between faster recovery of cortisol levels with milder blunting of ACTH (and with it presumably other POMC peptides including endorphins with physiological consequences).

Appendix Section 3. Possible network topologies for the regulation of corticotroph and adrenal masses.

In this section we compare putative alternative topologies (interaction network architectures) for the regulation of tissue mass in the HPA axis. The experimentally observed interactions are the regulation of the pituitary corticotroph mass by CRH and the regulation of the adrenal cortex mass by ACTH. One could imagine other interactions between the hormones and gland masses. We were specifically interested in asking which topologies provide the features of the HPA hormones discussed here: exact adaptation of x_2, hypercortisolemia during elevated stress for x_3, and the dysregulation phenomena shown in Figure 1.

For this purpose, we consider all possible interactions between hormones and glands, where CRH, ACTH, and cortisol, can activate either the production or removal of cell mass of either the pituitary corticotrophs or the cortisol-secreting adrenal cortex cells. We describe this by the general equations:

$$\frac{dC}{dt} = w_C C\left(x_1^{a_{1C}} x_2^{a_{2C}} x_3^{a_{3C}} - x_1^{b_{1C}} x_2^{b_{2C}} x_3^{b_{3C}}\right) \quad [1]$$

$$\frac{dA}{dt} = w_A A\left(x_1^{a_{1A}} x_2^{a_{2A}} x_3^{a_{3A}} - x_1^{b_{1A}} x_2^{b_{2A}} x_3^{b_{3A}}\right) \quad [2]$$

where all of the powers have values of 0 or 1. The 12 powers give a total of $2^{12} = 4096$ circuits. Since the adrenal cortex cannot sense hypothalamic CRH which is secreted into a private portal vein system directly to the pituitary, we set $a_{1A} = b_{1A} = 0$. This results in $2^{10} = 1024$ circuits. We solved the fixed point analytically, to find that only 464 have a fixed point, and 111 of these have a stable positive fixed point. Of these, we excluded the circuits where $a_{iC} = b_{iC}$ or $a_{iA} = b_{iA}$, since these do not affect the sign of Eq. 1, 2 and therefore do not affect whether or not they have the mismatch property. Finally, only 6 circuits show exact adaptation for x_2, as well as hypercortisolemia at high levels of input u. For all 6 circuits, Eq. 2 is $\frac{dA}{dt} = w_A A(x_2 - 1)$. Eq. 1 can be one of the following: (i) $\frac{dC}{dt} = w_C C(x_1 - 1)$, (ii) $\frac{dC}{dt} = w_C C(x_1 - x_2)$, (iii) $\frac{dC}{dt} = w_C C(x_1 - x_3)$, (iv) $\frac{dC}{dt} = w_C C(x_1 - x_2 x_3)$, (v) $\frac{dC}{dt} = w_C C(x_1 x_2 - 1)$, (vi) $\frac{dC}{dt} = w_C C(x_1 x_2 - x_3)$. Of these circuits only two circuits show the mismatch property after prolonged stress. These are circuit (i) which represents the experimentally observed interactions, and circuit (v) in which x_2 participates with x_1 to control corticotroph mass, in an ultrashort feedback loop. We conclude that the observed mass control interactions in the HPA axis are among the very few options that capture the observed phenomena.

Appendix Section 4. Analysis of the dynamical compensation properties of the HPA model.

Here we analyze the dynamical compensation properties of the general (un-normalized) equations of the HPA axis (Eq. 6-10 in Methods). The model equations are, writing x_1, x_2 and x_3 for CRH, ACTH and cortisol:

$$\frac{dx_1}{dt} = k_1 u(t) \cdot M(x_3) \cdot G(x_3) - w_1 x_1 \quad [1]$$

$$\frac{dx_2}{dt} = k_2 C x_1 \cdot G(x_3) - w_2 x_2 \quad [2]$$

$$\frac{dx_3}{dt} = k_3 A x_3 - w_3 x_3 \quad [3]$$

$$\frac{dC}{dt} = C(k_C x_1 - w_c) \quad [4]$$

$$\frac{dA}{dt} = A(k_A x_2 - w_A) \quad [5]$$

The w_i parameters are the removal rates, and the k_i parameters are the hormone production rates. We note here that we focus on the slow timescale of weeks, and the rates k_1, k_2, k_3 do not affect the conclusions of the paper. By equating all derivatives to zero, the steady-state solution of the model is (for $x_3 \ll K_{GR}$):

$$x_{1,st} = \frac{w_P}{k_P}$$

$$x_{2,st} = \frac{w_A}{k_A}$$

$$x_{3,st} = \frac{k_1 k_P}{w_1 w_P} u$$

$$C_{st} = \frac{k_C w_2 w_A}{w_C k_2 k_A}$$

$$A_{st} = \frac{w_3 k_A \frac{u k_1 k_C}{w_1 w_C}}{k_3 w_A}$$

We next define dynamical compensation and test it in this model. A system has dynamical compensation with respect to parameter p and variable x, if for any input $u(t)$ and any constant value of p the dynamics of the variable x does not depends on p, provided the initial conditions are at steady-state (Karin *et al*, 2016). To rule out trivial cases, such as systems in which p does not affect the dynamics at all or is non-identifiable (Karin *et al*, 2017), we further require that when the system is out of steady-state, the output $x(t)$ for a given $u(t)$ *does* depend on the value of p.

A necessary condition for dynamical compensation is that the *steady-state* value of the variable x is independent of p. Thus, it is easy to rule out dynamical compensation when the steady state value depends on the parameter. To establish dynamical compensation for the rest of the cases, we used the method of Karin et al. (Karin *et al*, 2016) ,which employs transformed variables to prove invariance.

We find that in the HPA model many variables are dynamically compensated for the secretion rates k_i. For example, cortisol x_3 has dynamical compensation with respect to the secretion rates of C and A, and the proliferation rate of A. No variable, however, has dynamical compensation with respect to the removal rates w_i since they change the timescale of the dynamics.

	CRH x_1	$ACTH$ x_2	$CORT$ x_3	C	A
k_1	+	+			
k_2	+	+	+		+
k_3	+	+	+	+	
k_C		+			
k_A	+		+		
w_C		+			
w_A	+		+		

Table S1. Dynamical compensation in the HPA model for the case of $CORT \ll K_{GR}$. Compensated variables are in the columns and respective compensated parameters are in the rows. + marks represent pairs of dynamically compensated parameter and variable.

Note that the above table holds for the case where the GR is not activated ($CORT \ll K_{GR}$). In the more general case, where $CORT$ can be similar or larger than K_{GR}, the following table holds:

	CRH x_1	$ACTH$ x_2	$CORT$ x_3	C	A
k_2	+	+	+		+
k_3	+	+	+	+	
k_A	+		+		
w_A	+		+		

Table S2. Dynamical compensation in the HPA model for the general case. Compensated variables are in the columns and respective compensated parameters are in the rows. + marks represent pairs of dynamically compensated parameter and variable.

Of special importance are the parameters k_2 and k_3, because they are expected to vary physiologically. These hormone secretion parameters (per unit biomass and per unit upstream hormone) can vary with the metabolic state of the corticotrophs and adrenal cells, the number of receptors for the upstream hormone, neuronal inputs, cytokines and other factors. They also vary with blood volume because increased blood volume dilutes out blood hormone levels and effectively changes these parameters (which is inversely proportional to blood volume) (Karin *et al*, 2016).

Thus, dynamical compensation ensures a proper cortisol and ACTH response regardless of physiological changes that affect the specific secretion rates k_2 and k_3. It ensures that a given stress input u(t) provides an output time course of ACTH and cortisol which does not depend on the secretion parameters, provided the initial conditions including C and A masses are at steady state. The phenomena described in the main text are transients in which C and A have not yet reached steady state, resulting in blunted hormone responses to CRH tests. Long after the prolonged stress described in Figure 2,3, the system returns to steady state and responses return to normal.

References.

Cohen S, Janicki-Deverts D, Doyle WJ, Miller GE, Frank E, Rabin BS & Turner RB (2012) Chronic stress, glucocorticoid receptor resistance, inflammation, and disease risk. *Proc. Natl. Acad. Sci.* **109:** 5995–5999

Karin O, Alon U & Sontag E (2017) A Note On Dynamical Compensation And Its Relation To Parameter Identifiability. *bioRxiv***:** 123489

Karin O, Swisa A, Glaser B, Dor Y & Alon U (2016) Dynamical compensation in physiological circuits. *Mol. Syst. Biol.* **12:** 886

Merkulov VM, Merkulova TI & Bondar NP (2017) Mechanisms of brain glucocorticoid resistance in stress-induced psychopathologies. *Biochem. Mosc.* **82:** 351–365